

March 2022

Effects of acid hydrolyzed chitosan derivatives on MHV infection

Krishna Sharma
University of South Florida

Follow this and additional works at: <https://digitalcommons.usf.edu/etd>



Part of the [Medicinal Chemistry and Pharmaceutics Commons](#)

Scholar Commons Citation

Sharma, Krishna, "Effects of acid hydrolyzed chitosan derivatives on MHV infection" (2022). *USF Tampa Graduate Theses and Dissertations*.
<https://digitalcommons.usf.edu/etd/10355>

This Thesis is brought to you for free and open access by the USF Graduate Theses and Dissertations at Digital Commons @ University of South Florida. It has been accepted for inclusion in USF Tampa Graduate Theses and Dissertations by an authorized administrator of Digital Commons @ University of South Florida. For more information, please contact digitalcommons@usf.edu.

Effects of Acid Hydrolyzed Chitosan Derivatives on MHV Infection

by

Krishna Sharma

A thesis submitted in partial fulfillment
of the requirements for the degree of
Master of Science in Pharmaceutical Nanotechnology
Department of Pharmaceutical Sciences
Taneja College of Pharmacy
University of South Florida

Major Professor: Subhra Mohapatra Ph.D.
Eleni Markoutsa Ph.D.
Shyam Mohapatra Ph.D.

Date of Approval:
March 15th, 2022

Keywords: Atomic Force Microscopy (AFM), Fourier Transform Infrared Spectroscopy (FTIR), 17CL1 fibroblast cell lines, green fluorescent proteins (GFP)

Copyright © 2022, Krishna Sharma

Table of Contents

List of Figures.....	iii
List of Tables.....	iv
Abstract.....	v
Chapter One Background.....	1
1.1 Coronaviruses	1
1.2 Current Treatments against Coronaviruses	2
1.3 Chitosan	4
1.4 Hypothesis:.....	7
Chapter 2: Materials and Methods	8
2.1 Acid Hydrolysis Procedure on Chitosan	8
2.2 Analysis of the control and hydrolyzed samples	8
2.2.1 IR Spectra:.....	8
2.2.2 Atomic Force Microscopy.....	9
2.3 Cell Culture.....	9
2.4 Cell Viability Assay	9
2.5 Viral Infection.....	10
2.6 Analysis of the experiment.....	10
Chapter 3: Results and Discussion	11
3.1 Hydrolysis of the samples.....	11
3.2 Characterization of the non-hydrolyzed chitosan using FTIR	11
3.2.2 Characterization of the chitosan samples using AFM	12
3.2.3 Toxicity of unhydrolyzed and hydrolyzed chitosan on 17CL1	12
3.2.4 In vitro Experiment.....	13
3.3 IR results of the original chitosan sample	14
3.4 Toxicity study of the sample	19
3.5 Results of the chitosan on the MHV infected 17CL1 cells at 72 hours	21
Chapter 4: Conclusion and Future Direction	25

Chapter 5: References 26

List of Figures

Figure 1: A figure depicting the antiviral properties of chitosan and their method of functioning.	6
Figure 2: Effects of Acid Hydrolysis on Chitosan. The acid causes the polymer to break into smaller chains. This was used to break down the chain to be used in the experiment.	6
Figure 3: Effects of Base Hydrolysis on Chitosan. The base hydrolysis removes the acetyl groups turning chitin into chitosan.	7
Figure 4: a and b: IR Spectra of the unhydrolyzed chitosan and IR spectra of the unhydrolyzed labeled with letters	14
Figure 5: A labelling of chitosan and its functional groups that are described in table 1.	15
Figure 6: Example of relevant modifications of the graph needed to calculate the values for degree of acetylation using the Domzy method (Domszy & Roberts, 1985).	16
Figure 7: AFM results of both hydrolyzed and non-hydrolyzed samples at different magnification.	17
Figure 8: Toxicity study of the non-hydrolyzed and hydrolyzed chitosan on the cell lines used.	19
Figure 9a and b: (a) Inhibition of viral infection using both hydrolyzed and non-hydrolyzed chitosan and (b) the results of the imagej fluorescence to find the amount of viral expression difference between control and samples.	21

List of Tables

Table 1: A Comparison Between MHV and SARS-CoV-2..... 3

Table 2: A table showing the different functional groups of chitosan and their corresponding wavelengths. The different letters are labelled on figure 5. 15

Table 3: The absorbance and the final value of degree of acetylation of the samples using the Domzy method (Domszy & Roberts, 1985). 16

Abstract

Coronaviruses have recently been under significant scrutiny due to the ongoing covid-19 pandemic that began in Wuhan, China, and subsequently spread to the rest of the world. Chitosan is a common chemical from crustaceans that has several desirable properties due to being biodegradable, non-toxic, and, most importantly, cheap. It also exhibits anti-viral properties, which is the focus of these experiments. We tested the toxicity of the chitosan on cell lines to see how much chitosan the cells can tolerate. We hydrolyzed the chitosan in acid, and the chitosan fibrils added cell lines to see if the anti-viral properties increased in those batches compared to the original. Afterwards, we tested the different chitosan samples against the mouse hepatitis virus to limited success when hydrolyzed for less than an hour. The hydrolyzed samples showed some greater efficacy than the starting material at concentrations 4 and 40 $\mu\text{g/ml}$

Chapter One Background

1.1 Coronaviruses

With the recent covid-19 pandemic that is still raging worldwide at the time of writing this introduction, coronaviruses have been under significant scrutiny and are being researched for better understanding (Zheng, 2020). Coronaviruses are single-stranded, enveloped, positive-strand RNA viruses (Weiss & Navas-Martin, 2005). The SARS-CoV-2 pandemic has proven to be a grave threat as it has infected and killed several million people globally (Ahsan, Javed, Bratty, Alhazmi, & Najmi, 2020).

Covid-19 is a coronavirus from Wuhan, China that in November 2019 that began to infect human cells through its spike protein binding to the ACE-2 receptor. By binding ACE-2 the protein cannot bind to Angiotensin II, which causes a buildup in fluid in the lungs or edemas which is the cause of several deaths (Zwaveling, Gerth van Wijk, & Karim, 2020). Attempts to block the binding of the spike protein to the ACE-2 receptor are possible to prevent covid-19 infections. (Vitiello, Pelliccia, & Ferrara, 2021). In the past 2 decades alone, there have been several outbreaks of zoonotic coronaviruses, such as SARS-CoV-1 (SARS) in East Asia during the early 2000s and Middle Eastern Respiratory Virus (MERS) in the Middle East during the 2010s (Perlman, 2020); SARS coming from pangolins and MERS coming from camels. It is currently unknown from which animal SARS-CoV-2 originates. There have been several treatments to remediate covid-19, such remdesivir and several vaccines have been developed and deployed in various nations

after early 2021 and even had emergency FDA approval in the United States (Beigel et al., 2020; D. Singh, Wasan, Mathur, & Gupta, 2020).

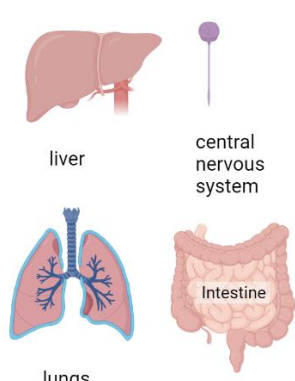
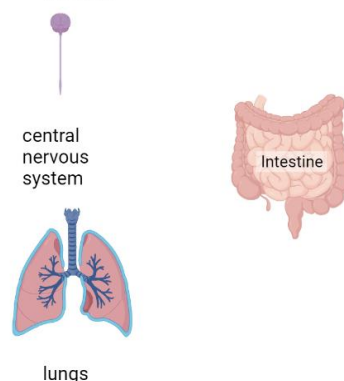
Therefore, due to the importance of coronaviruses in the current time this thesis will test against one. The virus that will be used in this experiment is mouse hepatitis virus (MHV). MHV and SARS-CoV-2 share the same genus and has been postulated to help find possible treatments to covid (Robert W. Körner, Mohamed Majjouti, Miguel A. Alejandro Alcazar, & Esther Mahabir, 2020). MHV is a BSL-2 virus which means that it was able to be used within the confines of the laboratory. As well, MHV has several similarities to SARS-CoV-2 Certain strains of MHV like the organs affected and other parts shown in Table 1 (R. W. Körner, M. Majjouti, M. A. A. Alcazar, & E. Mahabir, 2020). have also been altered to express green fluorescent proteins (GFP). GFPs are proteins that when expressed will fluoresce a green color depending on the amount of protein expressed. This fluorescence makes it easier to determine infection in cell lines through using the microscope.

1.2 Current Treatments against Coronaviruses

Several drugs have been thought to work against the covid-19 infection such as remdesivir or hydroxychloroquine (Ahsan et al., 2020; Andreani et al., 2020; Arnold & Buckner, 2020; Arshad et al., 2020; Beigel et al., 2020; Costanzo, De Giglio, & Roviello, 2020; Fantini, Chahinian, & Yahi, 2020; Gautret, Lagier, Parola, Hoang, Meddeb, Mailhe, et al., 2020; Gautret, Lagier, Parola, Hoang, Meddeb, Sevestre, et al., 2020; Gendelman, Amital, Bragazzi, Watad, & Chodick, 2020; Juurlink, 2020; McKee, Sternberg, Stange, Laufer, & Naujokat, 2020; Million et al., 2020; Pastick et al., 2020; Saleh et al., 2020; D.

Singh et al., 2020; Song et al., 2020; Tu et al., 2020; Yao et al., 2020). Currently, several vaccines have been developed to treat the virus. For example, there has been a resurgence of covid-19 infections in nations with high vaccine turnout rates such as Israel, the United Kingdom, and the United States of America (Keehner et al., 2021). Since 2021, the FDA approved the usage of Molnupiravir from the company Merck to treat the virus (A. K. Singh, Singh, Singh, & Misra, 2021).

Table 1: A Comparison Between MHV and SARS-CoV-2

	MHV	SARS-CoV-2
Structure	Contains <ul style="list-style-type: none"> • Spike Protein • Envelope Protein • Nucleoprotein • Hemagglutinin Esterase 	Contains <ul style="list-style-type: none"> • Spike Protein • Envelope Protein • Nucleoprotein
Viral Receptor	CECAM1	ACE2
Organs affected	<ul style="list-style-type: none"> • Intestine • Liver • Lungs • Central nervous system <p>MHV targets in mice</p>  <p>The diagram for MHV targets in mice shows four anatomical illustrations: a liver, a central nervous system (represented by a brain and spinal cord), a pair of lungs, and a section of the intestine. Each illustration is connected to a purple dot representing the virus particle by a thin line.</p>	<ul style="list-style-type: none"> • Intestine • Lungs • Central nervous system <p>SARS-CoV-2 targets in humans</p>  <p>The diagram for SARS-CoV-2 targets in humans shows three anatomical illustrations: a central nervous system (represented by a brain and spinal cord), a pair of lungs, and a section of the intestine. Each illustration is connected to a purple dot representing the virus particle by a thin line.</p>

1.3 Chitosan

Chitosan is the de-acetylated form of chitin; the second most ubiquitous polymer in nature after cellulose, found in the exoskeletons of crustaceans and the cell walls of fungi. Primarily chitosan comes from crustaceans as this provides a significant source of chitin, making it abundant and cheap (Azuma, Osaki, Minami, & Okamoto, 2015; Sabir, Altaf, & Shafiq, 2019; Schmitz et al., 2019).

Chitosan actually refers to when chitin is 50% de-acetylated or more but the term is still used to refer to chitin that is more than 50% de-acetylated (Schmitz et al., 2019). Chitosan can be acquired and formed from discarded crustacean shells, as shown in fig. 2. Chitosan is manipulated through two different methods, acid (fig. 2), and base hydrolysis (Kasaai, Arul, & Charlet, 2013; Schmitz et al., 2019). Deacetylation is done by treating the chitin polymer with concentrated base such as NaOH, as shown in fig. 3. Degradation of the polymer into smaller chains can be done using two methods, either chemically with concentrated acid or hydrogen peroxide or enzymatically (Davydova et al., 2011). When chitosan is smaller than 20 monomers in length or under 3.9 kilodaltons, then they are considered oligomers (Gonçalves, Ferreira, & Lourenço, 2021). Given the abundance of the polymer, it is of great interest due to its affordability and its usefulness against various medical capabilities like antiviral or antibacterial properties (Davydova et al., 2011). For example, the degree of acetylation and the molecular weight of the chitosan have been proven to influence the function of the polymer; the function in question to try and influence is chitosan's antiviral properties (Davydova et al., 2011). The size of the polymer is determined by the number of sugar chains connected i.e., the monomer is a single chain, the dimer is a chain with 2 sugars, etc. The monomer of

chitosan is similar to glucose with an amine group replacing the 2nd carbon, hence the name glucosamine. Currently, the acetylated form of the monomer aka. N-acetyl Glucosamine is being tested as a treatment against covid- (Hassan, 2021). Degree of acetylation can be determined in a sample by comparing the absorbance of the chain at 345 cm⁻¹ and at 60 cm⁻¹; This value then divided by 1.33 will give the percentage of the chain with the acetyl group (Domszy & Roberts, 1985). However, another method, based on the ratio of the sample at 1320 cm⁻¹ and 1420 cm⁻¹ can be used instead (Brugnerotto et al., 2001). Both degree of acetylation and the size of the polymer affect the chemical properties of the chain; one being solubility, as the chitosan becomes more deacetylated and smaller, the chitosan chain is more soluble in water. If the chitosan chain is smaller than can be dissolved at a neutral pH, larger chains need to be dissolved in acidic environments, if they can be dissolved at all. Commercial chitosan is sold at different molecular weights where the large ones can be sold at over 300 kDa and low molecular weight can be sold at above 30 kDa.

Chitosan has applicability as an antiviral drug in both plants and animals due to its properties, although the mechanism is not well understood (Chirkov, 2002). Chitosan currently has exhibited antiviral properties effective against covid-19 in cell lines and in vivo mice models by inhibiting the virus from attaching to the ACE-2 receptor in the body (Alitongbieke et al., 2020). It also depicts general antiviral effects by binding to the viral structure, disrupting viral – cell receptor bonding, and attaching to the negative viral structure as show in figure 1 (Safarzadeh et al., 2021).

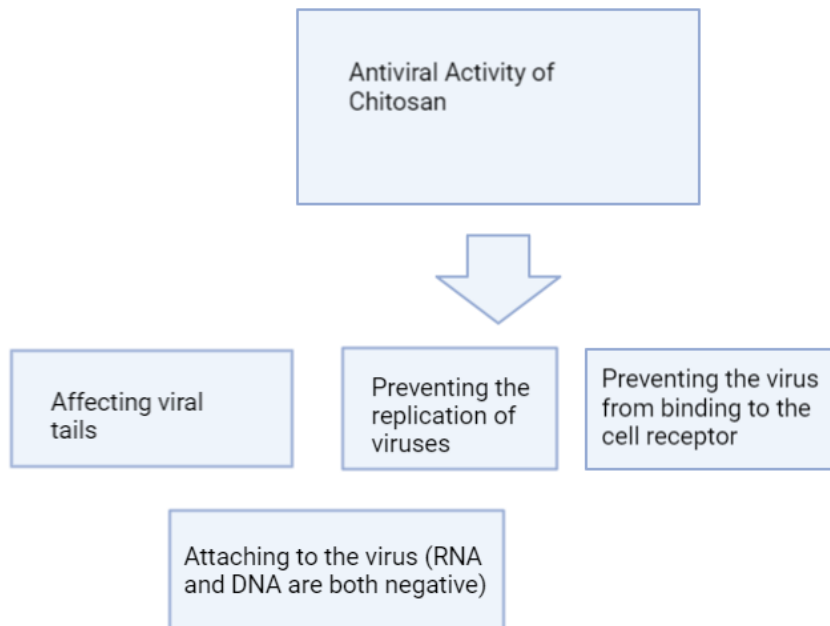


Figure 1: A figure depicting the antiviral properties of chitosan and their method of functioning.

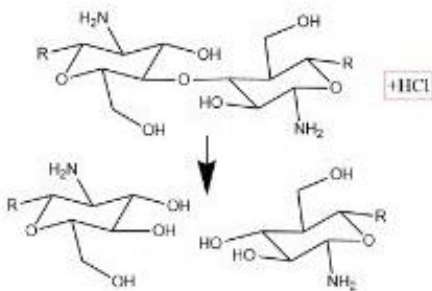


Figure 2: Effects of Acid Hydrolysis on Chitosan. The acid causes the polymer to break into smaller chains. This was used to break down the chain to be used in the experiment.

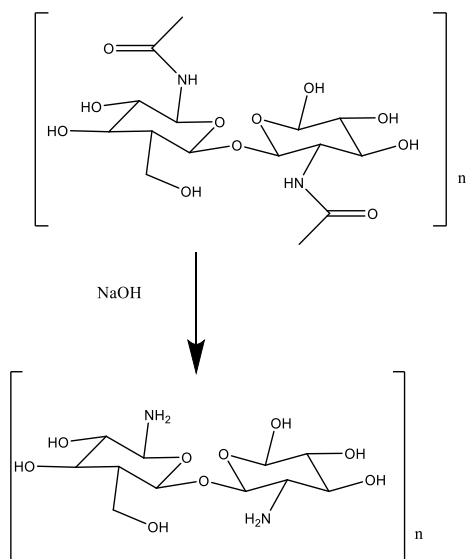


Figure 3: Effects of Base Hydrolysis on Chitosan. The base hydrolysis removes the acetyl groups turning chitin into chitosan.

1.4 Hypothesis:

We hypothesize that due to the literature's claims of higher efficacy with shorter chains of chitosan then using acid hydrolysis to break down the chitosan chains to form chitosan solutions will also increase the chitosan's antiviral properties. If the experiment proves this hypothesis in these cell lines, then the experiment will be repeated with other cell lines and other coronaviruses and in the animal models.

Chapter 2: Materials and Methods

2.1 Acid Hydrolysis Procedure on Chitosan

The original chitosan samples were dissolved in 2 molar hydrochloric acid for differing amounts of time. The samples were dissolved in times of multiples of 30 minutes until 120 minutes. This would give samples of the original, 30 minutes, 60 minutes, 90 minutes, and 120 minutes for a total of 5 samples of equal volume. Once the acid hydrolysis was completed the samples were then neutralized with NaOH to release the chitosan from solution. The samples were then centrifuged and decanted free of the liquid to just leave the solid particles left. These solid precipitates were then vacuumed free of any remaining liquid and then dissolved into 10 mg/ml stocks. These different stocks were then dissolved into several different concentrations that were used both for treatment and for toxicity studies. The stock was dissolved so that when 5 μ L of sample was added to a given well the concentration of the well would have 400 μ g/ml, 40 μ g/ml, 4 μ g/ml, and 0.4 μ g/ml.

2.2 Analysis of the control and hydrolyzed samples

2.2.1 IR Spectra:

Fourier-transform infrared spectroscopy works by emitting light to different chemical compounds which absorb the frequency at different wavelengths, these wavelengths correspond to different functional groups which is a useful tool to

characterize organic compounds. The degree of acetylation can be found using the FTIR method. FTIR works by just adding the sample to the reader and running the machine to see the spectra. The resonance of the different functional groups causes different signals which can be seen in the final spectra.

2.2.2 Atomic Force Microscopy

Atomic force microscopy or AFM works by measuring and imaging the topography of the sample. After hydrolyzing the sample, the AFM will show the difference between the hydrolyzed and the original chitosan samples by measuring the surface roughness of the samples on the substrate (Zhang et al., 2016).

2.3 Cell Culture

The cell line used in these experiments was a murine cell line 17CL1. This cell line is known for specifically growing coronaviruses such as MHV (Sawicki & Sawicki, 1990). The cells were grown on petri dishes with DMEM until confluent when they could then be used to plate 96 well plates. Once confluent the cells can then be plated for 5k per well.

2.4 Cell Viability Assay

Cell-titer glo[®] Luminescent Cell Viability Assay by Promega and imagej are what can measure the luminescence of the cell lines. Cell-titer glo[®] measures ATP production in cells by lysing the cell and reacting with oxyluciferin and this will be used to measure the toxicity of the different solutions. Imagej can measure the fluorescence of virus in the cell lines and can show the decrease of viral expression in tested cell lines or the percentage of infected cells can be found just by counting. With this data, graphpad and

t-tests can be used to test significance between the different treatments compared to the control (Xu et al., 2007).

2.5 Viral Infection

Once cells were plated and confluent on 96 well plates viral loads were formed to infect the lines. The experiments worked with 0.1 MOI or multiplicity of infection for each well. The viral load for each well can be determined by calculated the MOI multiplied by the number of wells multiplied by the number of cells per well. This gives the total number of viral particles needed which then can be divided by the plaque forming units to get how much of viral stock is needed for the experiment and dissolved in opti-mem solution. Once the cells were confluent the DMEM was removed, and viral solutions were added to the wells. The cells were then left to incubate with the virus for 72 hours. The steps to treatment with the particles were changed with regards to the viral infection depending on if it were pre-treating or post-treating.

2.6 Analysis of the experiment

After the cells have been infected and treated, they were analyzed with the Keyence microscope. 10 μ L of nuc-blue was added to each well to show the nuclei of each cell.

Chapter 3: Results and Discussion

3.1 Hydrolysis of the samples

During the hydrolysis of the sample the chitosan dissolved in the acid. The sample when removed and base was added precipitated out of sample.

3.2 Characterization of the non-hydrolyzed chitosan using FTIR

Characterization of the samples were done to see the differences between the chitosan samples that were hydrolyzed by the acid and the original. In order to characterize the original sample and find the functional groups and the degree of acetylation FTIR is used. All relevant functional groups are denoted in the table of figure 5. The FTIR showed that the IR spectra of the original sample, this sample would then need to be modulated to find the degree of acetylation. This would be done by finding the difference at the absorbance at 1420 from the base line of the two nearest peaks and the difference at the absorbance at 1320 from the baseline of the two nearest peaks of that value. Using the following formula, the degree of acetylation of the non-hydrolyzed sample was found to be ~20%. As well the spectra shown in figure 4 and figure 5 show that this sample is chitosan due to the functional groups shown in the spectra which are labelled as well in figure 5.

$$\left(\frac{\text{Modified Absorbance at 1320}}{\text{Modified Absorbance at 1420}} - 0.3822 \right) * \left(\frac{1}{0.03133} \right) = \text{degree of acetylation}$$

3.2.2 Characterization of the chitosan samples using AFM

The samples were also characterized with atomic force microscopy to see if the acid hydrolysis broke down the chitosan chains. AFM can be used to determine the molecular weight of samples or even find the general size of the samples. According to figures 7 and 8, the samples did break the chains as long chains are shown in the unhydrolyzed sample but little to no chains appear in the short chain photo. As the samples appear in the right side of the figures to not be large chains but instead either small samples or aggregations of small samples. In both figures pertaining to the comparison of the samples the long chains appear in the unhydrolyzed sample whereas these chains disappear in the hydrolyzed samples, in both $50 \times 50 \mu\text{m}^2$ and $4 \times 4 \mu\text{m}^2$.

3.2.3 Toxicity of unhydrolyzed and hydrolyzed chitosan on 17CL1

After the samples were characterized, they had to be tested for toxicity on the cell lines. This is done to see if the samples will be toxic to the cells as otherwise, they would not be viable treatments to viral infections. The samples were tested for toxicity by administering the samples at the relevant concentrations on the cell lines after they reach confluency. After they reached confluency at 72 hours, cell titer glo ® was added. After the samples were ran under cell titer glo ® the samples, the samples showed significant fluorescent concentrations on the cells at different concentrations that deviated from the control's luminescence as shown in figure 7. The samples turned out to be relatively non-toxic on the cell lines even at high concentrations, but there was a significant different at some concentrations for the unhydrolyzed samples. The hydrolyzed samples showed no significant difference at any concentration when compared to the control. Therefore,

samples can be tested at these higher concentrations to see if it will have any effect on the viral expression while not killing the cells.

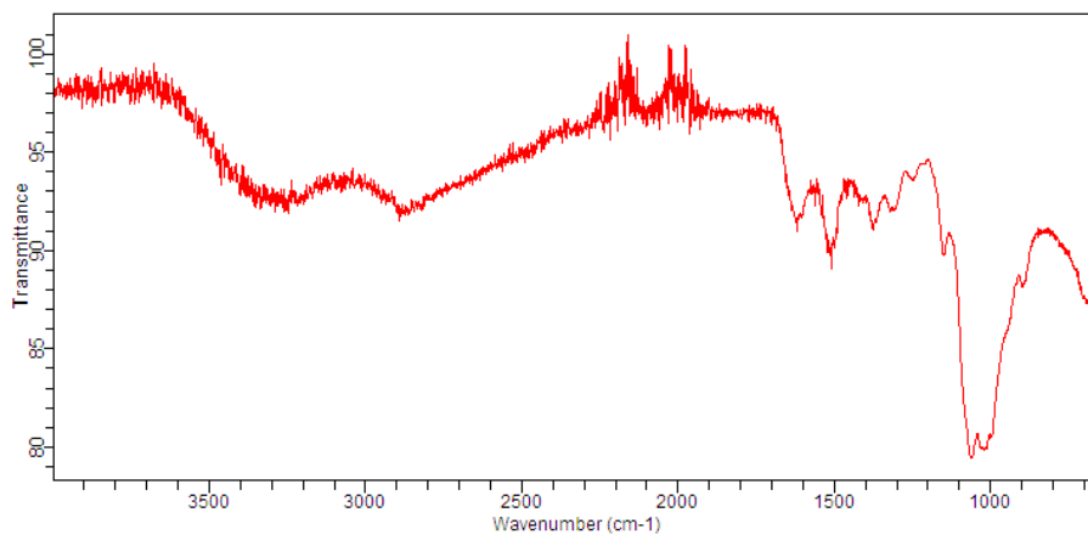
3.2.4 In vitro Experiment

Once the range of toxicity was determined, infections would begin. Cell lines were infected with MHV as 17CL1 is readily infected by that virus. The cell lines when infected with 0.1 MOI MHV ended up infected, especially after 48 and 72 hours of incubation. Some of the samples especially at the highest concentration show a decrease of viral expression compared to the control. Imagej was used to quantify both the viral expression and the number of cells in the different wells. The quantification of the viral infection and its difference from control is what is plotted in figure 5.

The 17CL1 cells were successfully infected with 0.1 MOI of MHV virus and were treated with the different chitosan mixtures. The MHV has been modified to fluoresce, so it fluoresces which makes it simple to count the number of cells that are infected. The blue fluorescence of the nuc-blue shows a better contrast to the MHV green. Photos were taken of each well to show the infection and its changes to the cell lines from 24-72 hours in 24-hour intervals. The changes in the infection will show the effects of the different samples on the infection. The cells were then counted to find the number of green, fluorescent cells divided by the blue cells. Both the green and blue were shown in each image which means that the number of infected and the number of cells would easily be counted and quantified in figure 10.

3.3 IR results of the original chitosan sample

a.



b.

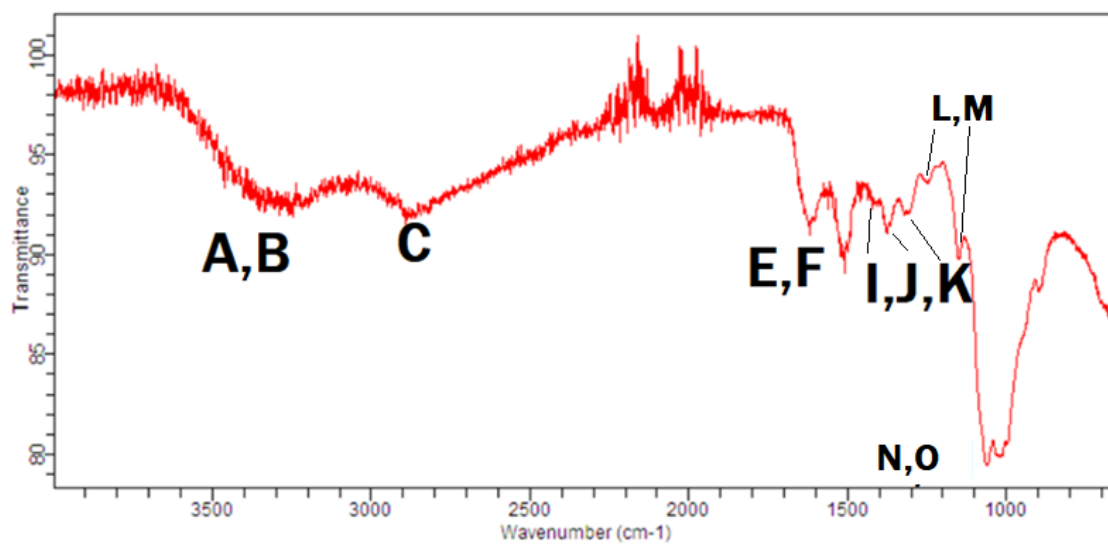


Figure 4: a and b: IR Spectra of the unhydrolyzed chitosan and IR spectra of the unhydrolyzed labeled with letters

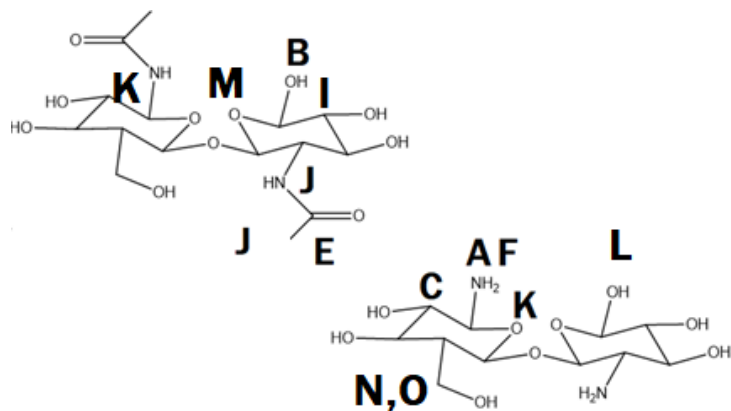


Figure 5: A labelling of chitosan and its functional groups that are described in table 1.

Table 2: A table showing the different functional groups of chitosan and their corresponding wavelengths. The different letters are labelled on figure 5.

Wavelength (cm ⁻¹)	Letter	Corresponding Group
3291–3361 cm	A, B	NH, OH stretching and hydrogen bonding
2921 and 2877	C	C-H symmetric/asymmetric stretching
1645	E	C=O stretching of amide
1589	F	N-H stretch of primary amine
1423, 1375	I, J	CH ₂ bending, CH ₃ symmetrical deformations
1325	K	C-N amide stretch
1260	L	Hydroxyl bending
1153	M	Asymmetrical stretch of C-O-C
1066, 1028	N, O	C-O stretching

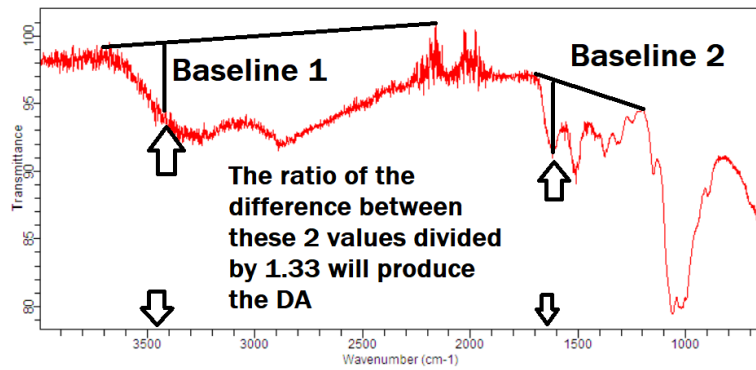


Figure 6: Example of relevant modifications of the graph needed to calculate the values for degree of acetylation using the Domzy method (Domszy & Roberts, 1985).

Table 3: The absorbance and the final value of degree of acetylation of the samples using the Domzy method (Domszy & Roberts, 1985).

Absorbance Wavelength 1/cm	Absorbance at frequency	Ratio after calculation
1419.707928	92.60180933	19.54098343
1320	92.08499963	
1419.707928	91.66066371	19.62124863
1320	91.3796064	
1419.707928	86.21161658	19.49246427
1320	85.59941976	
1419.707928	81.02738772	19.45277507
1320	80.35125006	
1419.707928	84.9080399	19.47321698
1320	84.25389884	
average	standard deviation	
19.51614%	0.067236635%	

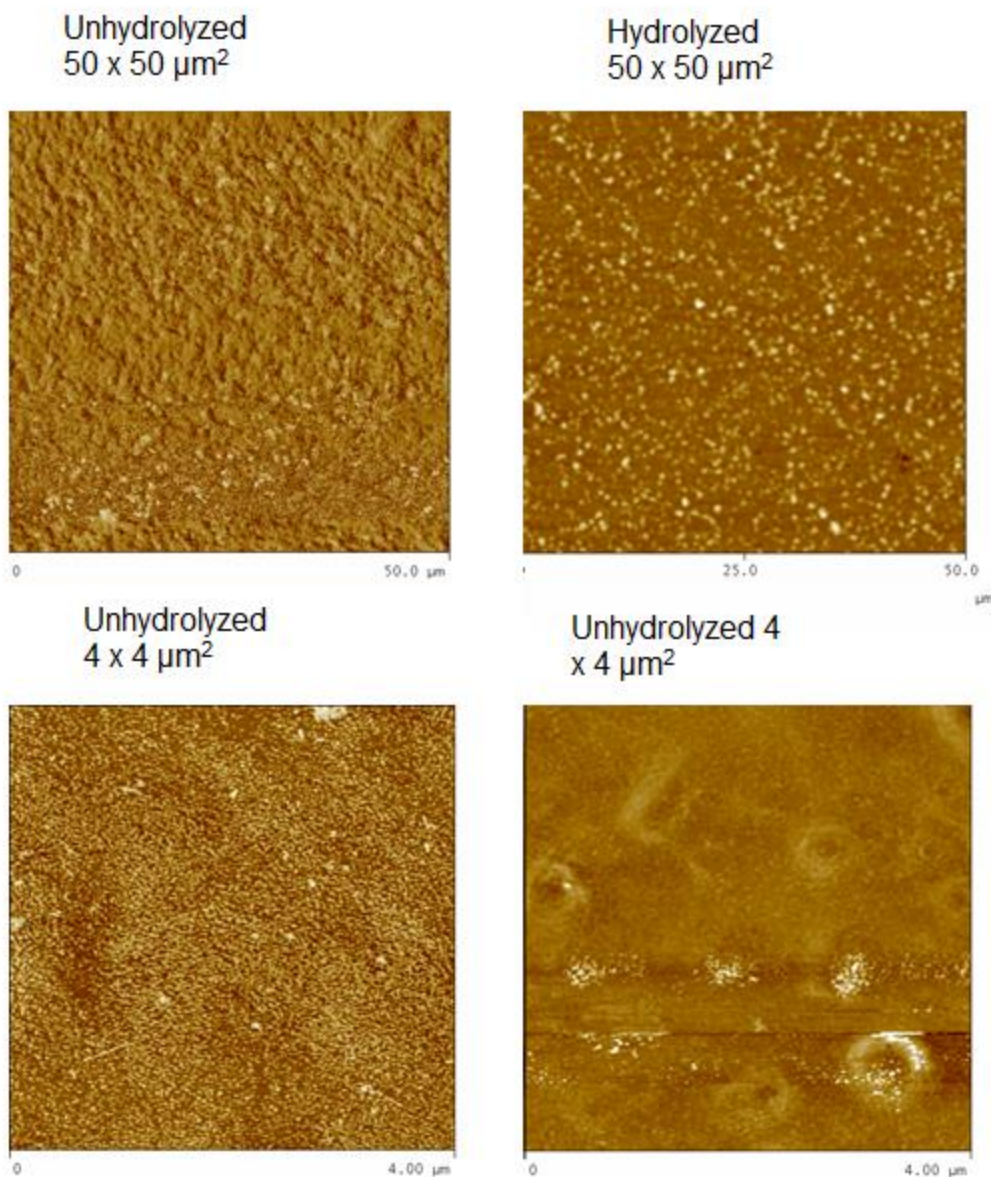


Figure 7: AFM results of both hydrolyzed and non-hydrolyzed samples at different magnification. AFM results for unhydrolyzed (left) and hydrolyzed (right) 50 x 50 μm² and 4 x 4 μm².

The left side images show more dense collections of chitosan that aggregate compared to the right which do not have many samples. Either due to low size or carried over due to condensation in the atmosphere. This therefore shows that the sample undergoes a

chemical change between and after acid hydrolysis. AFM was done to show the differences between the starting material and the hydrolyzed material. Although the size could not be characterized from the images the difference between the left and right images showcases the different samples when analyzed under the AFM. There are large and more compact samples on the left samples compared to the right. Although the size of the samples could not be determined with these images, the difference between the samples can be illustrated.

3.4 Toxicity study of the sample

Toxicity Study results of the different solutions on the 17CL1 cells by measuring the fluorescence. All samples and their concentrations are compared to the control.

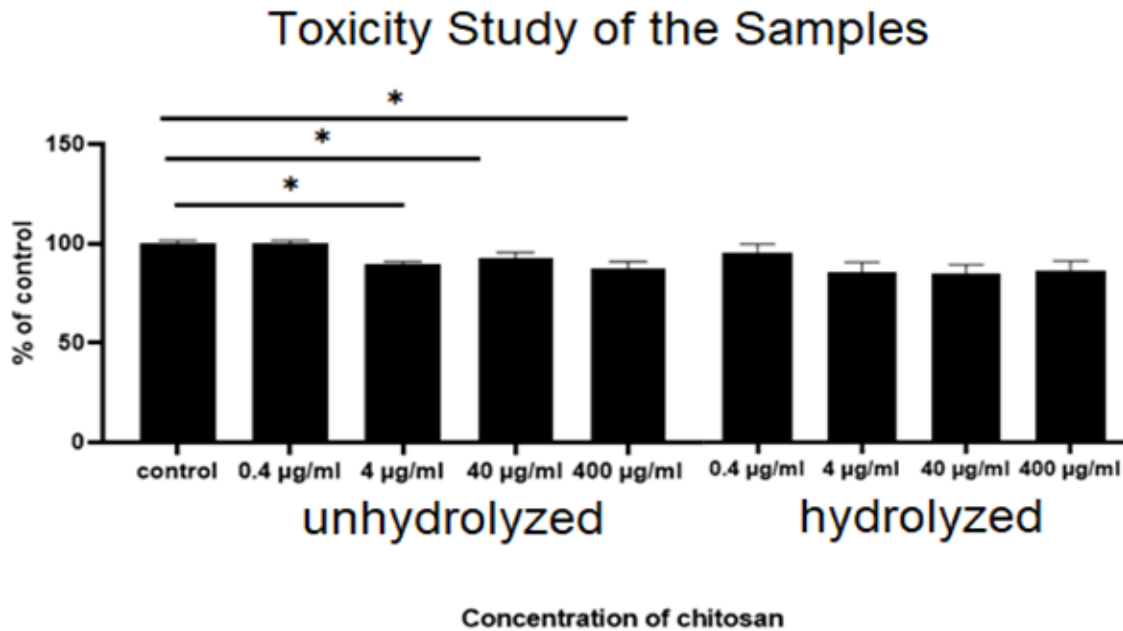


Figure 8: Toxicity study of the non-hydrolyzed and hydrolyzed chitosan on the cell lines used.

The cells were treated with different concentrations of chitosan and then left to incubate for 48 hours. The luminescence was then determined to find the cell viability to the samples. For the non-hydrolyzed samples only 0.4 ug/ml was non-toxic to the cell lines. For the oligomers none of the samples were determined to be toxic despite some decrease in cell viability. For both samples all samples above 4 ug/ml decreased the viability of the cell lines compared to the control.

The experiment was completed in order to test the viability of the cell lines with the different chitosans used. To do so, appropriate amounts of chitosan were administered until the desired concentration in each well. Doing so the results were shown in figure 12 where significance was determined between the highest three concentrations of the 10kda chitosan when compared to the control.

3.5 Results of the chitosan on the MHV infected 17CL1 cells at 72 hours

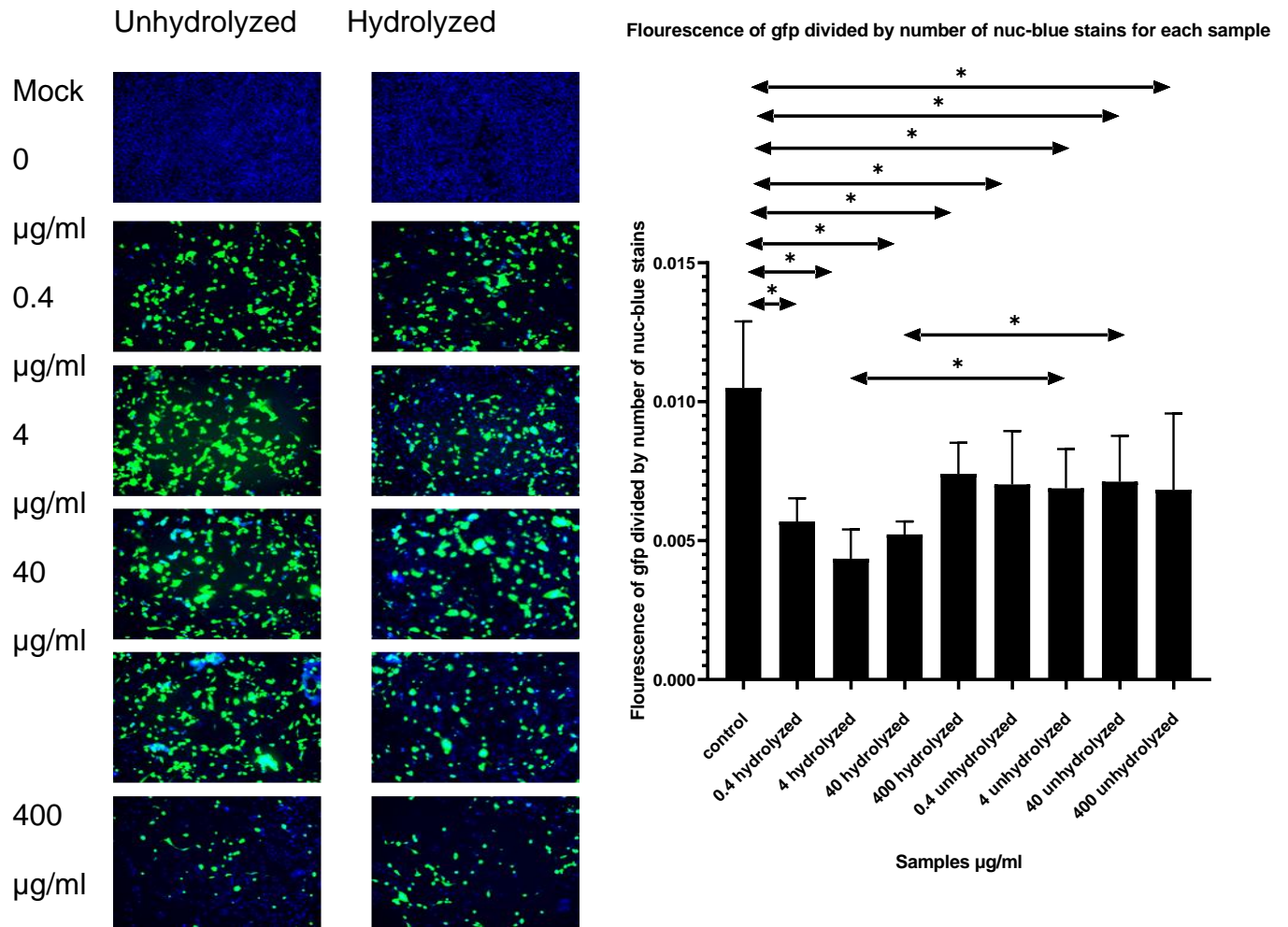


Figure 9a and b: (a) Inhibition of viral infection using both hydrolyzed and non-hydrolyzed chitosan and (b) the results of the imagej fluorescence to find the amount of viral expression difference between control and samples.

Representative images used to measure fluorescence of the 17CL1 cells infected with 0.1 MOI MHV. These show the effects of the chitosan on the cell lines, and which have more expression than others. For a general trend the higher the concentration the lower

the viral expression as shown by more blue and less green shown in the final 2 rows. MHV infected cells being to die as shown in parts of the trials having less blue intensity. Cell densities also appear to be higher in 0.4 $\mu\text{g/ml}$ and 4 $\mu\text{g/ml}$ despite having more green intensity. (b) All samples are significant with $p < 0.01$ and is a graphical interpretation of the samples at different concentrations and hydrolyzation.

The images were taken in order to quantify the different effects between the different samples. Images like these in figure 13 were what were used to find the viral expression of the cell lines. Counting the green and blue fluorescence with image J and dividing the two graphed is figure 14. The samples were then tested with ANOVA compared to the control and all samples had a significant effect ($p < 0.01$). Concentrations between the different samples that did have a significant difference ($p < 0.05$) include only the 4 $\mu\text{g/ml}$ concentration.

3.7 Discussion:

According to the AFM figures (7 and 8), the samples are clearly different, implying a change in the chitosan structure between the different samples. This makes sense as it is expected for acid to hydrolyze the chitosan chain as well, when testing the samples on the cell lines the cells showed toxicity for the unhydrolyzed but not the hydrolyzed. This is one of the benefits of chitosan, its non-toxicity, so these results seem normal. The shorter chains do provide some possible benefit as they did not show toxicity to the cell lines when compared to the control. Increasing the number of hydrolyzed samples makes the second solution batches have a higher molarity than the original batches despite having the same mass per volume. When the unhydrolyzed sample is hydrolyzed, the number of molecules increases. This makes sense as a chitosan chain with 10 monomers hydrolyzed can have 10 smaller resultant monomers maximum. The increase of resultant materials provides more molecules to disrupt either viral replication or the viral protein complex. This increase of molecules in the solution could potentially lead to increased antiviral effects. ANOVA statistical tests were done to test the significance and the significance showed that the hydrolyzed chitosan was less toxic than the unhydrolyzed samples. As for the results of the samples on the MHV infected cells, all the samples at each concentration were significantly different from the control, which was expected due to chitosan's antiviral properties. However, both the concentration at 40 and 4 $\mu\text{g/ml}$ turned out to have a significant difference between each other; implying that the acid hydrolyzed samples did have a stronger effect on viral expression than the original chitosan. Therefore, the hypothesis can be accepted for 40 and 4 $\mu\text{g/ml}$ but rejected at the other concentrations. Coupled with the fact that the hydrolyzed samples had no toxic

effect on the cell lines, at 40 and 4 $\mu\text{g/ml}$ the hydrolyzed sample is more effective on the viral expression of 17CL1 cell lines than the original chitosan. The viral expression appears to increase at higher concentrations which could be due to more starting material being in the higher concentration samples, but this would require future focus to conclusively determine the cause of this mechanism.

Chapter 4: Conclusion and Future Direction

The experiments showed some promise in using acid to break down chitosan to be used for treatment against viruses. The hydrolyzed samples were not toxic to the cells, which was expected due to chitosan's low toxicity to cell lines, but at higher concentrations, the unhydrolyzed samples did show toxic effects to the cell line. The samples that underwent acid hydrolysis and at middle concentrations appeared to have significant antiviral effects on the cell lines over the original unhydrolyzed chitosan. However, more experiments have to be done to confirm its efficacy on MHV infection in vivo and coronaviruses in other cell lines. The mechanism of action of chitosan as an antiviral could be further studied.

Chapter 5: References

- Ahsan, W., Javed, S., Bratty, M. A., Alhazmi, H. A., & Najmi, A. (2020). Treatment of SARS-CoV-2: How far have we reached? *Drug Discov Ther*, *14*(2), 67-72. doi:10.5582/ddt.2020.03008
- Alitongbieke, G., Li, X.-m., Wu, Q.-C., Lin, Z.-C., Huang, J.-F., Xue, Y., . . . Pan, Y.-T. (2020). Study on β -Chitosan against the binding of SARS-CoV-2S-RBD/ACE2. *bioRxiv*, 2020.2007.2031.229781. doi:10.1101/2020.07.31.229781
- Andreani, J., Le Bideau, M., Duflot, I., Jardot, P., Rolland, C., Boxberger, M., . . . Raoult, D. (2020). In vitro testing of combined hydroxychloroquine and azithromycin on SARS-CoV-2 shows synergistic effect. *Microb Pathog*, *145*, 104228. doi:10.1016/j.micpath.2020.104228
- Arnold, S. L. M., & Buckner, F. (2020). Hydroxychloroquine for Treatment of SARS-CoV-2 Infection? Improving Our Confidence in a Model-Based Approach to Dose Selection. *Clin Transl Sci*, *13*(4), 642-645. doi:10.1111/cts.12797
- Arshad, S., Kilgore, P., Chaudhry, Z. S., Jacobsen, G., Wang, D. D., Huitsing, K., . . . Zervos, M. (2020). Treatment with hydroxychloroquine, azithromycin, and combination in patients hospitalized with COVID-19. *Int J Infect Dis*, *97*, 396-403. doi:10.1016/j.ijid.2020.06.099
- Azuma, K., Osaki, T., Minami, S., & Okamoto, Y. (2015). Anticancer and anti-inflammatory properties of chitin and chitosan oligosaccharides. *Journal of functional biomaterials*, *6*(1), 33-49. doi:10.3390/jfb6010033

- Beigel, J. H., Tomashek, K. M., Dodd, L. E., Mehta, A. K., Zingman, B. S., Kalil, A. C., . . . Lane, H. C. (2020). Remdesivir for the Treatment of Covid-19 — Final Report. *New England Journal of Medicine*, 383(19), 1813-1826. doi:10.1056/NEJMoa2007764
- Brugnerotto, J., Lizardi, J., Goycoolea, F. M., Argüelles-Monal, W., Desbrières, J., & Rinaudo, M. (2001). An infrared investigation in relation with chitin and chitosan characterization. *Polymer*, 42(8), 3569-3580. doi:[https://doi.org/10.1016/S0032-3861\(00\)00713-8](https://doi.org/10.1016/S0032-3861(00)00713-8)
- Chirkov, S. (2002). The antiviral activity of chitosan. *Applied Biochemistry and Microbiology*, 38(1), 1-8.
- Costanzo, M., De Giglio, M. A. R., & Roviello, G. N. (2020). SARS-CoV-2: Recent Reports on Antiviral Therapies Based on Lopinavir/Ritonavir, Darunavir/Umifenovir, Hydroxychloroquine, Remdesivir, Favipiravir and other Drugs for the Treatment of the New Coronavirus. *Curr Med Chem*, 27(27), 4536-4541. doi:10.2174/0929867327666200416131117
- Davydova, V. N., Nagorskaya, V. P., Gorbach, V. I., Kalitnik, A. A., Reunov, A. V., Solov'eva, T. F., & Ermak, I. M. (2011). Chitosan antiviral activity: Dependence on structure and depolymerization method. *Applied Biochemistry and Microbiology*, 47(1), 103-108. doi:10.1134/S0003683811010042
- Domszy, J. G., & Roberts, G. A. (1985). Evaluation of infrared spectroscopic techniques for analysing chitosan. *Die Makromolekulare Chemie: Macromolecular Chemistry and Physics*, 186(8), 1671-1677.

- Fantini, J., Chahinian, H., & Yahi, N. (2020). Synergistic antiviral effect of hydroxychloroquine and azithromycin in combination against SARS-CoV-2: What molecular dynamics studies of virus-host interactions reveal. *Int J Antimicrob Agents*, 56(2), 106020. doi:10.1016/j.ijantimicag.2020.106020
- Gautret, P., Lagier, J. C., Parola, P., Hoang, V. T., Meddeb, L., Mailhe, M., . . . Raoult, D. (2020). Hydroxychloroquine and azithromycin as a treatment of COVID-19: results of an open-label non-randomized clinical trial. *Int J Antimicrob Agents*, 56(1), 105949. doi:10.1016/j.ijantimicag.2020.105949
- Gautret, P., Lagier, J. C., Parola, P., Hoang, V. T., Meddeb, L., Sevestre, J., . . . Raoult, D. (2020). Clinical and microbiological effect of a combination of hydroxychloroquine and azithromycin in 80 COVID-19 patients with at least a six-day follow up: A pilot observational study. *Travel Med Infect Dis*, 34, 101663. doi:10.1016/j.tmaid.2020.101663
- Gendelman, O., Amital, H., Bragazzi, N. L., Watad, A., & Chodick, G. (2020). Continuous hydroxychloroquine or colchicine therapy does not prevent infection with SARS-CoV-2: Insights from a large healthcare database analysis. *Autoimmun Rev*, 19(7), 102566. doi:10.1016/j.autrev.2020.102566
- Gonçalves, C., Ferreira, N., & Lourenço, L. (2021). Production of Low Molecular Weight Chitosan and Chitooligosaccharides (COS): A Review. *Polymers*, 13(15), 2466. doi:10.3390/polym13152466
- Hassan, A. E. (2021). An observational cohort study to assess N-acetylglucosamine for COVID-19 treatment in the inpatient setting. *Ann Med Surg (Lond)*, 68, 102574. doi:10.1016/j.amsu.2021.102574

- Juurlink, D. N. (2020). Safety considerations with chloroquine, hydroxychloroquine and azithromycin in the management of SARS-CoV-2 infection. *Cmaj*, *192*(17), E450-e453. doi:10.1503/cmaj.200528
- Kasaai, M. R., Arul, J., & Charlet, G. (2013). Fragmentation of chitosan by acids. *TheScientificWorldJournal*, *2013*, 508540-508540. doi:10.1155/2013/508540
- Keehner, J., Horton, L. E., Binkin, N. J., Laurent, L. C., Pride, D., Longhurst, C. A., . . . Torriani, F. J. (2021). Resurgence of SARS-CoV-2 Infection in a Highly Vaccinated Health System Workforce. *New England Journal of Medicine*, *385*(14), 1330-1332. doi:10.1056/NEJMc2112981
- Körner, R. W., Majjouti, M., Alcazar, M. A. A., & Mahabir, E. (2020). Of Mice and Men: The Coronavirus MHV and Mouse Models as a Translational Approach to Understand SARS-CoV-2. *Viruses*, *12*(8). doi:10.3390/v12080880
- Körner, R. W., Majjouti, M., Alcazar, M. A. A., & Mahabir, E. (2020). Of Mice and Men: The Coronavirus MHV and Mouse Models as a Translational Approach to Understand SARS-CoV-2. *Viruses*, *12*(8), 880.
- McKee, D. L., Sternberg, A., Stange, U., Laufer, S., & Naujokat, C. (2020). Candidate drugs against SARS-CoV-2 and COVID-19. *Pharmacol Res*, *157*, 104859. doi:10.1016/j.phrs.2020.104859
- Million, M., Lagier, J. C., Gautret, P., Colson, P., Fournier, P. E., Amrane, S., . . . Raoult, D. (2020). Early treatment of COVID-19 patients with hydroxychloroquine and azithromycin: A retrospective analysis of 1061 cases in Marseille, France. *Travel Med Infect Dis*, *35*, 101738. doi:10.1016/j.tmaid.2020.101738

- Pastick, K. A., Okafor, E. C., Wang, F., Lofgren, S. M., Skipper, C. P., Nicol, M. R., . . . Boulware, D. R. (2020). Review: Hydroxychloroquine and Chloroquine for Treatment of SARS-CoV-2 (COVID-19). *Open Forum Infect Dis*, 7(4), ofaa130. doi:10.1093/ofid/ofaa130
- Perlman, S. (2020). Another Decade, Another Coronavirus. *New England Journal of Medicine*, 382(8), 760-762. doi:10.1056/NEJMe2001126
- Sabir, A., Altaf, F., & Shafiq, M. (2019). Synthesis and Characterization and Application of Chitin and Chitosan-Based Eco-friendly Polymer Composites. In Inamuddin, S. Thomas, R. Kumar Mishra, & A. M. Asiri (Eds.), *Sustainable Polymer Composites and Nanocomposites* (pp. 1365-1405). Cham: Springer International Publishing.
- Safarzadeh, M., Sadeghi, S., Azizi, M., Rastegari-Pouyani, M., Pouriran, R., & Haji Molla Hoseini, M. (2021). Chitin and chitosan as tools to combat COVID-19: A triple approach. *International journal of biological macromolecules*, 183, 235-244. doi:10.1016/j.ijbiomac.2021.04.157
- Saleh, M., Gabriels, J., Chang, D., Soo Kim, B., Mansoor, A., Mahmood, E., . . . Epstein, L. M. (2020). Effect of Chloroquine, Hydroxychloroquine, and Azithromycin on the Corrected QT Interval in Patients With SARS-CoV-2 Infection. *Circ Arrhythm Electrophysiol*, 13(6), e008662. doi:10.1161/circep.120.008662
- Sawicki, S. G., & Sawicki, D. L. (1990). Coronavirus transcription: subgenomic mouse hepatitis virus replicative intermediates function in RNA synthesis. *Journal of Virology*, 64(3), 1050-1056. doi:doi:10.1128/jvi.64.3.1050-1056.1990

- Schmitz, C., Auza, L. G., Koberidze, D., Rasche, S., Fischer, R., & Bortesi, L. (2019). Conversion of Chitin to Defined Chitosan Oligomers: Current Status and Future Prospects. *Marine drugs*, 17(8), 452. doi:10.3390/md17080452
- Singh, A. K., Singh, A., Singh, R., & Misra, A. (2021). Molnupiravir in COVID-19: A systematic review of literature. *Diabetes & Metabolic Syndrome: Clinical Research & Reviews*, 15(6), 102329. doi:<https://doi.org/10.1016/j.dsx.2021.102329>
- Singh, D., Wasan, H., Mathur, A., & Gupta, Y. K. (2020). Indian perspective of remdesivir: A promising COVID-19 drug. *Indian journal of pharmacology*, 52(3), 227-228. doi:10.4103/ijp.IJP_486_20
- Song, Y., Zhang, M., Yin, L., Wang, K., Zhou, Y., Zhou, M., & Lu, Y. (2020). COVID-19 treatment: close to a cure? A rapid review of pharmacotherapies for the novel coronavirus (SARS-CoV-2). *Int J Antimicrob Agents*, 56(2), 106080. doi:10.1016/j.ijantimicag.2020.106080
- Tu, Y. F., Chien, C. S., Yarmishyn, A. A., Lin, Y. Y., Luo, Y. H., Lin, Y. T., . . . Chiou, S. H. (2020). A Review of SARS-CoV-2 and the Ongoing Clinical Trials. *Int J Mol Sci*, 21(7). doi:10.3390/ijms21072657
- Vitiello, A., Pelliccia, C., & Ferrara, F. (2021). Drugs acting on the renin–angiotensin system and SARS-CoV-2. *Drug Discovery Today*, 26(4), 870-874. doi:<https://doi.org/10.1016/j.drudis.2021.01.010>
- Weiss, S. R., & Navas-Martin, S. (2005). Coronavirus pathogenesis and the emerging pathogen severe acute respiratory syndrome coronavirus. *Microbiol Mol Biol Rev*, 69(4), 635-664. doi:10.1128/membr.69.4.635-664.2005

- Xu, S., Dong, M., Liu, X., Howard, K. A., Kjems, J., & Besenbacher, F. J. B. j. (2007). Direct force measurements between siRNA and chitosan molecules using force spectroscopy. *93*(3), 952-959.
- Yao, X., Ye, F., Zhang, M., Cui, C., Huang, B., Niu, P., . . . Liu, D. (2020). In Vitro Antiviral Activity and Projection of Optimized Dosing Design of Hydroxychloroquine for the Treatment of Severe Acute Respiratory Syndrome Coronavirus 2 (SARS-CoV-2). *Clin Infect Dis*, *71*(15), 732-739. doi:10.1093/cid/ciaa237
- Zhang, H., Li, Y., Zhang, X., Liu, B., Zhao, H., & Chen, D. J. F. N. N. (2016). Directly determining the molecular weight of chitosan with atomic force microscopy. *2*(3), 123-127.
- Zheng, J. (2020). SARS-CoV-2: an Emerging Coronavirus that Causes a Global Threat. *Int J Biol Sci*, *16*(10), 1678-1685. doi:10.7150/ijbs.45053
- Zwaveling, S., Gerth van Wijk, R., & Karim, F. (2020). Pulmonary edema in COVID-19: Explained by bradykinin? *Journal of Allergy and Clinical Immunology*, *146*(6), 1454-1455. doi:10.1016/j.jaci.2020.08.038